

NOTCH AND DEFECT SENSITIVITY OF ADI IN TORSIONAL FATIGUE

B. Atzori, G. Meneghetti
 Department of Mechanical Engineering
 University of Padova
 Via Venezia, 1 – 35131 Padova (Italy)

ABSTRACT

This work presents an extension of the well known Kitagawa-Takahashi diagram valid for cracks subjected to mode I loading to the case of mode III loading. By considering the crack as a limit case of a notch characterised by a very small tip radius and taking advantage of the N-SIF stress parameter for describing the local stress field close to the notch tip, the diagram is extended in order to encompass also U- and V-shaped notches. The notch opening angle and notch acuity, defined as the ratio between the notch depth and the notch tip radius, can be arbitrary.

After presenting the adopted analytical expressions, the theoretical estimations are compared with the experimental results obtained from torsional fatigue tests on smooth and notches specimens in austempered ductile iron. An equation for fatigue strength estimations in presence of defect-like notches and crack-like notches having an arbitrary notch opening angle is proposed and validated by means of the available experimental results. Finally observations of the fracture surfaces and of the early fatigue crack propagation are presented.

Introduction

Recently Atzori et al. [1] analysed the sensitivity to defects and to standard U-shaped notches in axial fatigue of metallic materials commonly adopted in manufacturing engineering components and structures, like steels and aluminium alloys. By means of the proposed approach, the effect of any kind of geometrical discontinuity on the fatigue limit can be treated, such as small defects, cracks, sharp or crack-like U-notches and standard rounded U-notches characterised by an arbitrary notch tip radius. The diagram sketched in Figure 1 was proposed for fatigue limit estimations of a notch centred in an infinitely wide plate: it can be thought as the extension of the well known Kitagawa-Takahashi diagram valid for mechanically short and long cracks, in order to include also U-notches characterised by an arbitrary notch acuity a/ρ , being a the notch depth and ρ the notch tip radius.

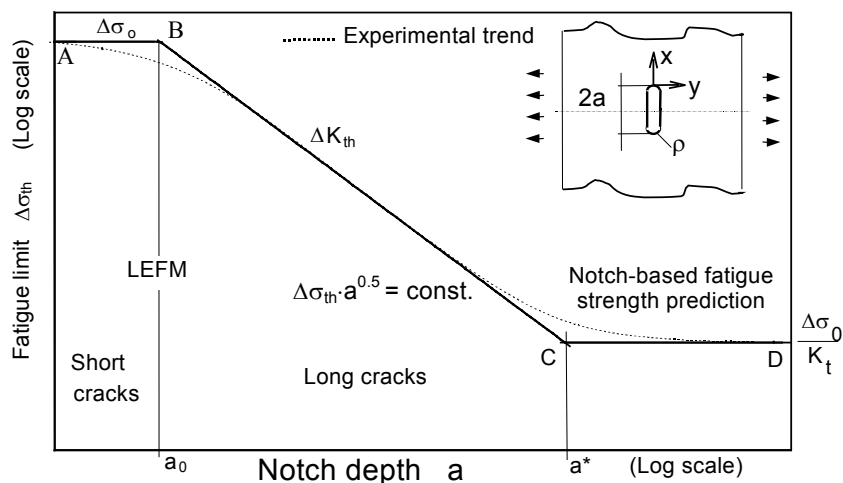


Figure 1. Fatigue limit for a U-notch characterised by an arbitrary acuity a/ρ (separation between short and long cracks based on a_0 has to be considered a simplified rule).

In summary, a crack was considered as the limit case of a standard U-notch notch characterised by a small notch tip radius. The variation of the fatigue limit of such a notch (in terms of gross nominal stress range $\Delta\sigma_{g,th}$) was analysed while varying its absolute dimensions, but keeping the geometry as a constant. Three asymptotic straight lines were then generated, which are separated by two characteristic lengths, i.e. the El Haddad-Smith-Topper length parameter a_0 , defined as:

$$a_0 = \frac{1}{\pi} \left(\frac{\Delta K_{th}}{\Delta\sigma_0} \right)^2 \quad (1)$$

and the characteristic length $a^*=K_t^2 \cdot a_0$. K_t is the elastic stress concentration factor referred to the gross section, ΔK_{th} the threshold range of the stress intensity factor and $\Delta\sigma_0$ the material fatigue limit. If the notch depth is lower than the material parameter a_0 then the presence of the notch will not affect the material fatigue limit; if the notch depth is between a_0 and a^* then the fatigue limit will be estimated by the LEFM criterion $\Delta K = \Delta K_{th}$; if the notch depth is greater than a^* then the classic criterion based on K_t will apply. The smooth transition shown by the experimental data from one regime to the other has been named "defect sensitivity" and "notch sensitivity" close to a_0 and a^* , respectively [1].

In order to extend the previous diagram to real components an effective notch dimension a_{eff} has to be introduced [1]:

$$a_{eff} = \frac{1}{\pi} \left(\frac{K_I}{\sigma_g} \right)^2 \quad (2)$$

In order to perform the fatigue limit estimations by means of the previous model (i) two material parameters are needed, i.e. the material fatigue limit $\Delta\sigma_0$ and the threshold range of the Stress Intensity Factor ΔK_{th} and (ii) one linear elastic stress analysis has to be performed in order to define the effective reference dimension from expression (2). Validation of the diagram reported in Figure 1 is documented in [1], while recently the criterion has been extended also to V-shaped notches, characterised by arbitrary opening angles and notch tip radii [2].

Aim of the present work is to extend the criterion summarised by Figure 1 also to torsional fatigue. In the next paragraph the model will be presented and then will be validated by means of experimental fatigue tests conducted on smooth and notched specimens in austempered ductile iron.

Analytical preliminaries

According to the local approach [2, 3 and references quoted therein, 4, 5], the fatigue strength of V-shaped notches characterised by a null tip radius can be made to depend on the Notch-Stress intensity Factor (N-SIF), which quantifies the local stress field intensity. In the case of Mode I loading, the relevant N-SIF was defined by Gross and Mendelson [6] as:

$$K_1 = \sqrt{2\pi} \lim_{r \rightarrow 0} [\sigma_{\theta\theta}(r, \theta = 0) r^{1-\lambda_1}] \quad (3)$$

where σ_{rr} and $\sigma_{\theta\theta}$ are the stress components in a polar frame of reference centred at the notch tip, as depicted in Figure 2a.

By extending the definition of K_1 [7], the N-SIF stress parameter for mode III loading can be defined as:

$$K_3 = \sqrt{2\pi} \lim_{r \rightarrow 0} [\tau_{\theta z}(r, \theta = 0) r^{1-\lambda_3}] \quad (4)$$

according to the symbols shown in Figure 2b. In the previous definitions (3) and (4), λ_1 is the eigenvalues in William's equations [8], while λ_3 is its natural extension to mode III elastic problems. In particular, referring to Figure 2b, exponent λ_3 is given by [9]:

$$\lambda_3 = q^{-1} \quad \text{being} \quad q = 2 \cdot \left(1 - \frac{\alpha}{\pi} \right) \quad (5)$$

The shear stress component $\tau_{\theta z}$ shown in Figure 2b can now be expressed as:

$$\tau_{\theta z} = \frac{K_3}{\sqrt{2 \cdot \pi \cdot r^{1-\lambda_3}}} \cdot \cos(\lambda_3 \cdot \theta) \quad (6)$$

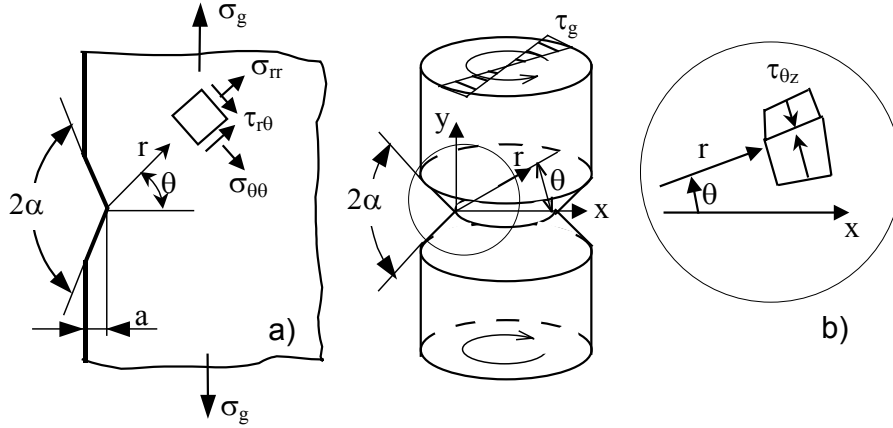


Figure 2. Definition of stress components for mode I (a) and mode III (b) loading.

An engineering expression for K_3 involving a nominal stress and a reference dimension of the component can be given, similarly to the well known expressions of the SIF adopted in LEFM studies [10]:

$$K_3 = k_3 \cdot \tau_g \cdot a^{1-\lambda_3} \quad (7)$$

where k_3 is a non-dimensional coefficient depending on the overall component's geometry, τ_g is the gross nominal shear stress quoted in figure 2b and a is the notch depth.

When applied at fatigue limit conditions, eq. (7) delivers the fatigue limit of the component containing a sharp V-shaped notch:

$$\Delta\tau_{g,th} = \frac{\Delta K_{3,th}}{k_3 \cdot a^{1-\lambda_3}} \quad (8)$$

where $\Delta K_{3,th}$ is thought as a characteristic material parameter for a given notch opening angle and load ratio R , defined as the ratio between the minimum and the maximum applied nominal shear stress. This assumption is consistent with the classical concept of threshold value of the Stress Intensity Factor adopted in LEFM.

Eq. (8) represent a straight line in the double logarithmic diagram reported in Figure 3. If a suitable effective length parameter $a_{eff,t}$, defined as:

$$a_{eff,t} = \left(\frac{K_3}{\tau_g} \right)^{\frac{1}{1-\lambda_3}} \quad (9)$$

is adopted in the abscissa then a unique line is obtained, whatever the component geometry and, consequently, the shape coefficient k_3 . The effective length $a_{eff,t}$ can be calculated by means of a linear elastic stress analysis, using the finite element method. Expression (9) is the equivalent for the case of torsion loading of the previous expression (2) valid for axial loading.

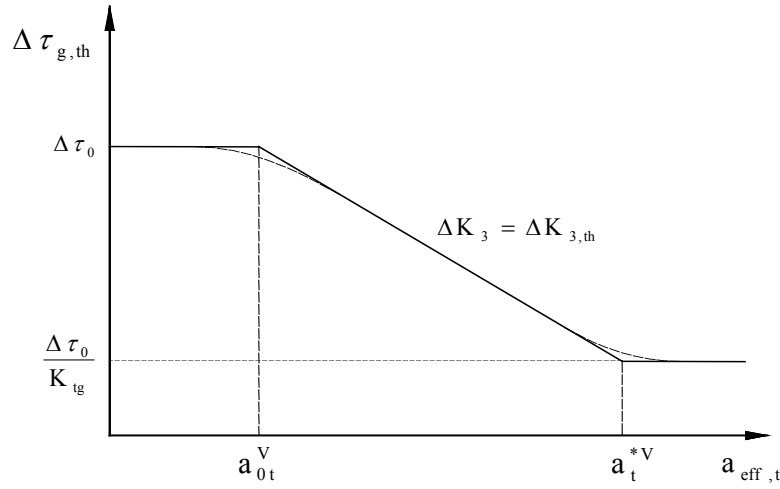


Figure 3. Plot of the torsional fatigue limit for components weakened by V-notches.

Similarly to the diagram presented in Figure 1, the fatigue limit for torsion loading given by eq. (8) can be bounded on the upper side by the material fatigue limit $\Delta\tau_0$, which cannot be exceeded, and on the lower side by the K_t -based fatigue limit $\Delta\tau_0/K_t$. Then two characteristic length can be defined in torsional fatigue, namely a_{0t}^V and a_t^{*V} . The former is defined as:

$$a_{0t}^V = \left(\frac{\Delta K_{3,th}}{\Delta\tau_0} \right)^{\frac{1}{1-\lambda_3}} \quad (10)$$

and is an extension of the El Haddad-Smith-Topper length parameter a_0 given by expression (1), while the latter is given by:

$$a_t^{*V} = a_{0t}^V \cdot K_t^{\frac{1}{1-\lambda_3}} \quad (11)$$

Three regions can then be schematically singled out in Figure 3. If $a_{eff,t} < a_{0t}^V$, then the presence of a (small) notch does not lower the fatigue limit with respect to the material torsion fatigue limit. If $a_{0t}^V < a_{eff,t} < a_t^{*V}$, the fatigue limit is determined by the condition that the N-SIF equals the threshold value, which is thought as a material property, i.e. $\Delta K_3 = \Delta K_{3,th}$. If $a_{eff,t} > a_t^{*V}$, then the fatigue limit can be predicted by applying the classic Notch Mechanics criterion, i.e. $\Delta\tau_{g,th} = \Delta\tau_0/K_t$. The smooth transition zones around a_{0t}^V and a_t^{*V} characterize the sensitivity to defects and notches, respectively.

Experimental test results and discussion

Specimens were machined from cast Lynchburg cylinders (diameter = 25 mm, length = 300 mm) made of in EN-GJS 800-8 (code: ADI 900) austempered ductile cast iron (tensile strength $\sigma_R = 900$ MPa, yield strength $\sigma_Y = 500$ MPa, elongation after fracture $A = 8\%$). The chemical composition of the material is reported in table 1. After casting the Lynchburg specimens, the microstructure composition was about 85% pearlite and 15% ferrite while the mean size of the graphite nodules was 22 μm . After the austempering heat treatment, about 30% of retained austenite was present in the microstructure, which resulted in a hardness value equal to 280 HB. Then, both smooth and notched specimens were machined according to the geometries listed in Table 2 for a total number of 6 geometries and 72 specimens subjected to fatigue tests. The adopted load ratio, defined as the ratio between the minimum and the maximum applied torque, was equal to -1 . The torsion fatigue tests were conducted by means of an MFL servo-hydraulic torsional machine equipped with a 1100 Nm load cell operating between 5 and 15 Hz.

During the fatigue tests the torque vs angular displacement signals were monitored and the tests were interrupted when the torsional stiffness drop was 40%. Moreover tests were stopped if the fatigue life exceeded $2 \cdot 10^6$ cycles. As a consequence,

the fatigue strength values considered in this work are not the fatigue limits $\Delta\tau_{g,th}$, but represents the fatigue strengths $\Delta\tau_{A,g}$ at a given number of cycle equal to $2 \cdot 10^6$ for a survival probability of 50%. Table 2 summarises also the fatigue test results: k is the inverse slope of the woehler curve while the parameter T_τ is the ratio between the fatigue strengths at 2 million cycles for a survival probability of 10% and 90%, respectively, both evaluated with a confidence level of 95%. Then T_τ quantifies the scatter of the experimental data.

C	Si	S	P	Mg	Mo	Mn	Cu	Ni	Cr
3,55÷3,56	2,44÷2,46	0,004	0,003	0,003-0,004	0,2÷0,25	0,1÷0,15	0,5÷0,7	0,9	0,02÷0,03

Table 1. Chemical composition of the austempered ductile iron

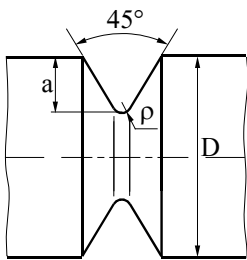
Notch geometries	D [mm]	a [mm]	ρ [mm]	K_t	$\Delta\tau_{A,g}$ (MPa)	k	T_τ
	20	0	/	1	574	12.4	1.12
	20	5	5	9.05	67	9.10	1.26
	20	5	1	12.5	54.8	6.37	1.19
	20	5	0.1	27.9	56.5	7.75	1.16
	20	2	0.1	7.62	223	6.70	1.14
	15	0.5	0.1	3.65	364	6.80	1.17

Table 2. Geometries of the tested series, elastic stress concentration factors referred to the gross section and summary of the fatigue test results

Figure 4 reports the fatigue test results in the diagram previously sketched in Figure 3. The material fatigue limit $\Delta\tau_0$ was obtained from the fatigue tests on smooth specimens and resulted equal to 574 MPa. The characteristic value $\Delta K_{3,A}$ was found by fitting the experimental results relative to the sharp V-notches (codes 20-5-0.1 and 20-2-0.1, respectively) by means of the theoretical eq. (8): Figure 4 highlights that the theoretical slope equal to 0.428, obtained from eq. (5) for a notch opening angle $2\alpha = \pi/4$, is in agreement with the trend of experimental results of the two series 2) and 3). The result was $\Delta K_{3,A} = 789 \text{ MPa} \cdot \text{mm}^{0.428}$ and, as aforementioned, this value is meant to be characteristic for the material, notch opening angle and load ratio adopted in the present work.

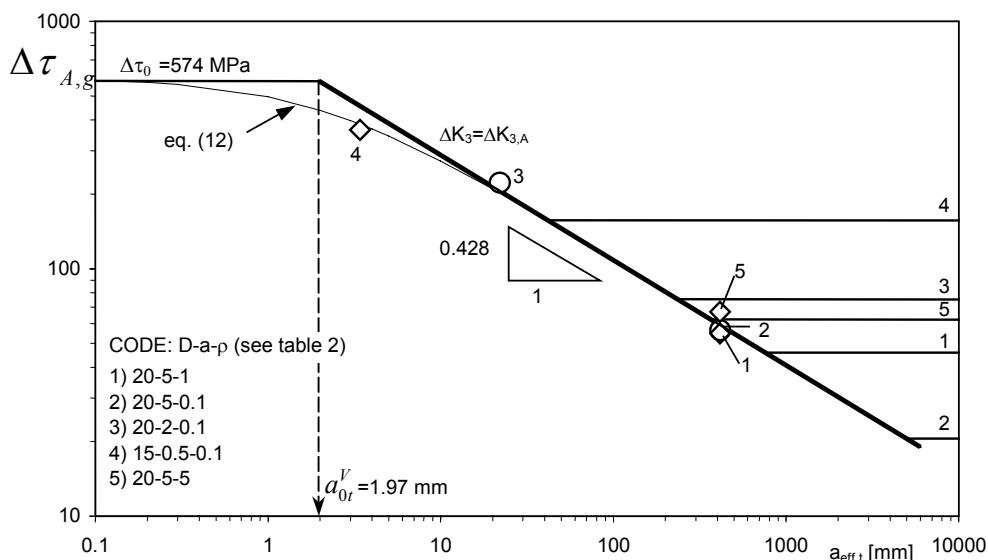


Figure 4. Fatigue test results and comparison with the theoretical slope equal to 0.428.

For each test serie the classic fatigue strength estimation based on K_t has been also reported in Figure 4. It can be noted that estimations based on K_t are much lower than the experimental value, thus supporting the previous assumption to consider the high cycle fatigue strength of series 2) and 3) governed by the N-SIF ΔK_3 . Concerning test series 1) and 5), it can be noted that the experimental data are located close to the knee point defined by the ΔK_3 - and the K_t -based lines, thus suggesting a small deviation of the fatigue behaviour from the two asymptotes in presence of some degree of notch sensitivity.

Finally test serie 4) contained a short circumferential notch thus simulating the presence of a “small” surface defect. Infact its fatigue strength is lower than that predicted by both the $\Delta \tau_0$ and the $\Delta K_{3,A}$ lines, according to the short crack behaviour highlighted in the classic Kitagawa diagram valid for axial loading. In order to extend our previous criterion [2], the following equation is now proposed for the estimation of the defect sensitivity of a material under torsional loading:

$$\Delta \tau_{A,g} = \frac{\Delta K_{3,A}}{\left(a_{\text{eff},t} + a_{0t}^V\right)^{1-\lambda_3}} \quad (12)$$

Eq. (12) is plotted in Figure 4 and shows a good agreement with the experimental point obtained from test serie 4).

Investigation of fatigue damage evolution

Torsional stiffness was monitored during fatigue tests from the load cell and position sensor RVDT signals so that typical trends could be derived, depending on the notch geometry. Figure 5 reports the relative torsional stiffness (K =actual torsional stiffness, K_i = torsional stiffness measured at the beginning of the fatigue test) as a function of the relative fatigue life for three notch geometries. In the case of short circumferential notches (code 15-0.5-0.1) the measured stiffness was practically unchanged for about 90% of the total fatigue life and then it begins to decrease quite rapidly. This behaviour was also observed for smooth specimens. In the case of the most deep and sharp notch (code 20-5-0.1) the stiffness begins to decrease after about 20% of the fatigue life and the curve decreases gradually up to 80% of the fatigue life; then the stiffness loss increases faster and faster up to final failure. These data are consistent with the observed experimental behaviour concerning the macro-crack propagation phase, which was seen to take a higher fraction of the total fatigue life in the case of deep and sharp notches with respect to the case of blunt or short notches. Similar phenomena have been observed also in carbon steels [11].

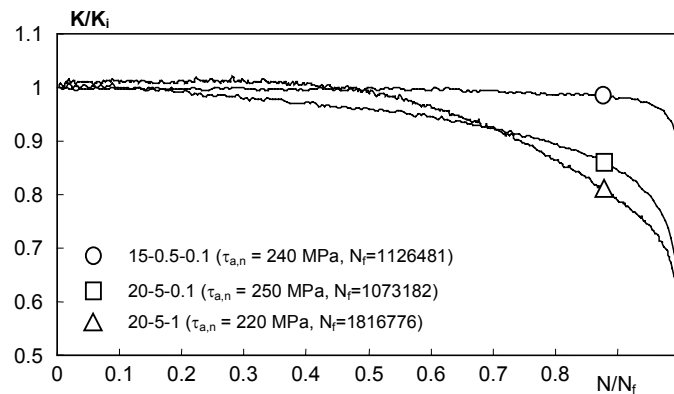


Figure 5. Typical torsional stiffness curves experimentally measured for different notch geometries.

Different evolution of the fatigue damage was also observed by considering the same notch geometry, but comparing tests conducted at high or low load levels. As an example, by taking into account the severely notches specimens (code 20-5-0.1) it was observed that multiple crack initiation sites are present along the circumferential notch tip at high load levels. Then macro crack propagation develops on planes oriented at 45° with respect to the specimen's longitudinal axis. As a consequence the fracture surface is factory roof shaped, as shown in Figure 6b. At low load levels a factory roof fracture surface was also observed, but there are much less crack initiation sites than in the previous case so that longer crack paths can develop on the 45° planes. This results in higher peaks and deeper valleys in the fracture surface, as shown in Figure 6a.

Generally speaking the same phenomenon was observed in specimens having a short circumferential notch (code 15-0.5-0.1), but at fatigue lives of the order of 1 million cycles cracks were observed to propagate also in the gross section of the specimen.

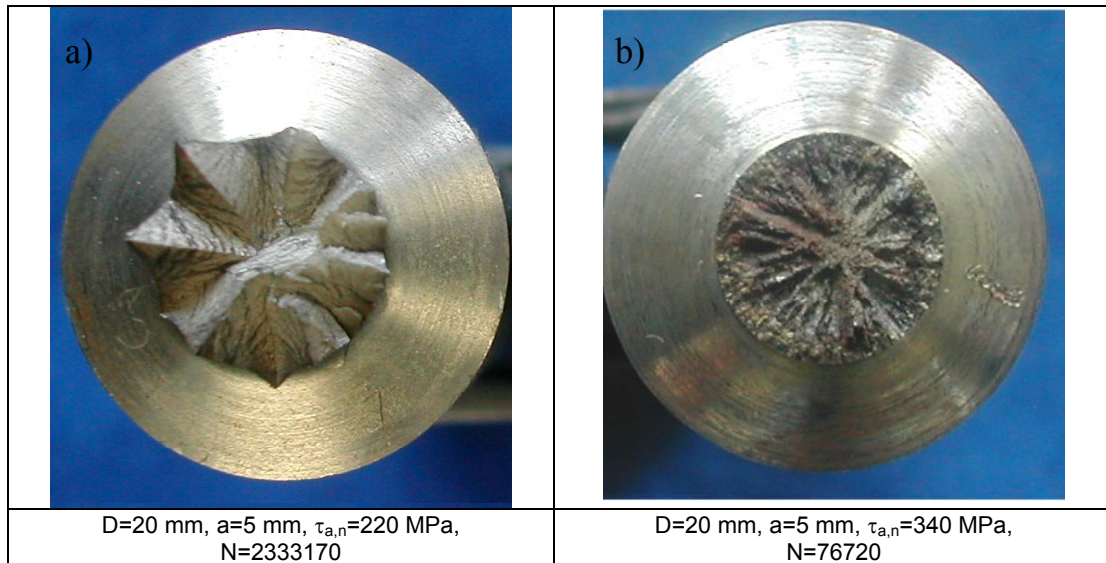


Figure 6. Fracture surface for severely notched specimens at long (a) or short fatigue life (b).

Additionally, observations conducted by means of the Scanning Electron Microscope enabled us to investigate the early crack propagation phase. As an example, Figure 7 shows small cracks (about 50 μm long) initiated after $2 \cdot 10^6$ cycles from a graphite nodule at the tip of the 5-mm-deep notch having a root radius equal to 0.1 mm. It is seen that initiation planes are oriented at 45° with respect to the specimen longitudinal axis. Then even if the experimental results were summarised in terms of the mode III N-SIF (ΔK_3), from a micromechanical point of view crack initiation and short crack propagation is mode I-controlled.

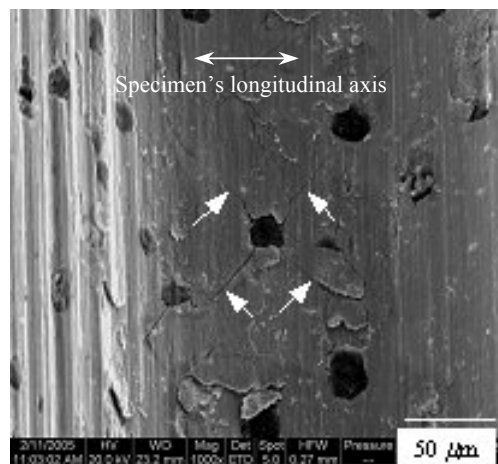


Figure 7. Early crack propagation from a graphite nodule.

Conclusions

A fatigue strength assessment criterion for components subjected to torsion loading has been presented and validated by means of experimental fatigue tests conducted on smooth and notched specimens in austempered ductile iron by adopting a load ratio equal to -1 . The criterion can be summarised by means of a diagram valid at the fatigue limit (or for a given high cycle fatigue life), where the sensitivity of the material to defect and notches are represented as transition zones between three different fatigue regimes: full notch sensitivity, Notch-Stress Intensity Factor based mechanics and material fatigue limit. According to the present experimental results the transition between N-SIF based mechanics and full notch sensitivity seems to be rather abrupt, then following quite closely the knee point formed by the reference theoretical models. An El-Haddad type equation (eq. 12) is proposed in order to account for defect- and crack-like notches having an arbitrary notch opening angle.

Finally by means of SEM observation on sharp V-shaped notches, it was seen that fatigue cracks initiated from graphite nodules located at the tip of sharp notches and along planes oriented at 45° with respect to the specimen longitudinal axis: then for this material and loading conditions crack initiation and propagation is mode I dominated at a microscopic level.

References

1. Atzori, B., Lazzarin, P. and Meneghetti, G., "Fracture Mechanics and Notch Sensitivity", *Fatigue Fract. Engng Mater. Struct.*, **26**, 257-267 (2003).
2. Atzori, B., Lazzarin, P. and Meneghetti, G., "A Unified Treatment of the Mode I Fatigue Limit of Components Containing Notches or Defects", *Int. J. Fracture*, **133**, 61-87 (2005).
3. Atzori, B., Lazzarin, P. and Tovo, R., "Stress Field Parameters to Predict the Fatigue Strength of Notched Components", *J. Strain Analysis*, **34(6)**, 437-453 (1999).
4. Boukarouba, T., Tamine, T., Nui, L., Chemini, C. and Pluvinage, G., "The Use of Notch Stress Intensity Factor as a Fatigue Crack Initiation Parameter", *Engng Fracture Mech.*, **52**, 503-512 (1995).
5. Kihara, S. and Yoshii, A., "A Strength Evaluation Method of a Sharply Notched Structure by a new Parameter, 'the Equivalent Stress Intensity Factor'", *JSME International Journal* **34**, 70-75 (1991).
6. Gross, R. and Mendelson, A., "Plane Elastostatic Analysis of V-Notched Plates", *Int. J. Fract. Mech.*, **8**, 267-276 (1972).
7. Lazzarin, P., Sonsino, C.M. and Zambardi, R., "A Notch Stress Intensity Approach to Assess the Multiaxial Fatigue Strength of Welded Tube-To-Flange Joints Subjected to Combined Loadings", *Fatigue Fract. Engng Mater. Struct.* **27**, 127-140 (2004).
8. Williams, M.L., "Stress Singularities Resulting from Various Boundary Conditions in Angular Corners of Plates in Extension", *J. Appl. Mech.*, **19**, 526-528 (1952).
9. Qian, J. and Hasebe, N., "Property of Eigenvalues and Eigenfunctions for an Interface V-Notch in Antiplane Elasticity", *Eng. Fract. Mech.* **56(6)**, 729-734 (1997).
10. Murakami, Y., "Stress Intensity Factor Handbook", Ed.-in-chief Y. Murakami, Pergamon Press (1990).
11. Atzori, B., Lazzarin, P. and Quaresimin, M., "Fatigue Behaviour of a Sharply Notched Carbon Steel under Torsion", *Procs of the Fatigue Crack Paths FCP International Conference*, 2003.